



JAAS

---

**Rapid  $^{235}\text{U}/^{238}\text{U}$  Determination by Matrix Assisted Ionization–Time-of-Flight Mass Spectrometry**

Journal:	<i>Journal of Analytical Atomic Spectrometry</i>
Manuscript ID	JA-ART-09-2024-000346.R1
Article Type:	Paper
Date Submitted by the Author:	21-Oct-2024
Complete List of Authors:	Bowden, Shelby; Savannah River National Laboratory, Samperton, Kyle; Savannah River National Laboratory, Trace Nuclear Measurement Technology Group LaBone, Elizabeth; Savannah River National Laboratory Lawton, Haley; Savannah River National Laboratory Waldron, Abigail; Savannah River National Laboratory, Global Security Directorate Mannion, Joseph; Savannah River National Laboratory Wellons, Matthew; Savannah River National Laboratory, Nuclear Nonproliferation Division Mannion, Danielle; Savannah River National Laboratory

SCHOLARONE™  
Manuscripts

Cite this: DOI: 00.0000/xxxxxxxxxx

Rapid  $^{235}\text{U}/^{238}\text{U}$  Determination by Matrix Assisted Ionization–Time-of-Flight Mass Spectrometry

Received Date  
Accepted Date

Shelby Bowden,<sup>\*ab</sup> Kyle M. Samperton,<sup>ab</sup> Elizabeth D. LaBone,<sup>a</sup> Haley B. Lawton,<sup>a</sup> Abigail M. Waldron,<sup>ab</sup> Joseph M. Mannion,<sup>a</sup> Matthew S. Wellons,<sup>a</sup> and Danielle R. Mannion<sup>ab</sup>

DOI: 00.0000/xxxxxxxxxx

Matrix-assisted ionization (MAI) of inorganic analytes is a nascent research domain that holds promise for rapid, potentially facility-deployable analytical applications. We present results of MAI uranium isotopic analysis ( $^{235}\text{U}/^{238}\text{U}$ ) obtained on the timescale of minutes utilizing simple sample preparation and an ambient ionization time-of-flight mass spectrometer (ToF MS). Experimental MAI–ToF MS characterization of uranium Certified Reference Materials (CRMs) was used to establish method calibration and validate quantitative  $^{235}\text{U}/^{238}\text{U}$  determination spanning depleted, natural, and low-enriched uranium isotopic compositions. Secondary standard analyses with total uranium mass loadings of 5–500 ng per analysis yield accurate calibrated  $^{235}\text{U}/^{238}\text{U}$  results and relative uncertainties of 4.7–17.2% (approx.  $\pm$  95% confidence level), with weighted-mean uncertainties approaching 1.5%. This method permits accurate determination of uranium isotopic composition in a sample with uranium content as low as 200 pg for equal atom  $^{235}\text{U}/^{238}\text{U}$ . Instrument detection limits constrain the minimum uranium mass required to identify the presence of highly enriched uranium ( $\text{HEU} \geq 20\%$   $^{235}\text{U}$ ) as only 500 pg using the method presented here. MAI–ToF MS quantitation of relatively extreme isotope ratios ( $^{235}\text{U}/^{238}\text{U} \leq 0.01$ ) is limited by detection of minor  $^{235}\text{U}$  ( $\text{LoD}_{^{235}\text{U}/^{238}\text{U}} \approx 100$  pg  $^{235}\text{U}$ /analysis  $\approx$  10 ng total U/analysis), and subsequent method optimization is anticipated to further reduce these limits. These findings underscore the potential of MAI–ToF MS for isotopic characterization of uranium and other inorganic species for both basic and applied science.

1 Introduction

Uranium and plutonium isotopic measurements are an important tool for environmental monitoring<sup>1,2</sup>, nuclear forensics<sup>3,4</sup>, and nuclear safeguards applications<sup>5,6</sup>. These isotopes have been traditionally measured using high-precision mass spectrometry techniques such as thermal ionization mass spectrometry (TIMS<sup>7–9</sup>) and solution-based inductively coupled plasma-mass spectrometry (ICP-MS<sup>10,11</sup>). While these methods produce highly reliable and repeatable isotopic measurements, they are resource-intensive and costly, with extensive sample preparation/purification and stringent laboratory infrastructural requirements.<sup>12</sup> This aspect of conventional uranium isotopic analysis results in a lengthy and expensive process between sample collection in the field and isotopic measurement results. A group of alternative mass spectrometry techniques broadly referred to as ambient mass spectrometry has shown recent promise in generating rapid uranium analyses<sup>13–18</sup>. These methods include electrospray ionization (ESI<sup>13–17</sup>), atmospheric pressure

glow discharge (APGD<sup>19–23</sup>), paper spray ionization (PSI<sup>24–26</sup>), and matrix-assisted ionization (MAI<sup>18</sup>), and have the advantage of providing faster and cheaper means of characterizing species-of-interest in potentially austere environments<sup>27,28</sup>. Ambient ion sources rely on “soft” ionization<sup>27–31</sup>, and as such are relatively simple and robust compared to traditional mass spectrometric methods. Furthermore, ambient ionization instruments are characterized by straightforward hardware and operational requirements, best exemplified by their use for on-site clinical diagnosis in medical facilities by trained non-experts<sup>32–34</sup>.

MAI is one of the more recent and least understood ambient mass spectrometric phenomenon. This technique produces ions without a conventional ion source; instead, ions are generated by simply mixing sample with a specific chemical compound (i.e., MAI matrix) and exposing the mixture to vacuum<sup>18,28–30,35,36</sup>. Prior work has demonstrated the efficacy of MAI as a method for rapid uranium detection<sup>18</sup>; however, the applicability of MAI in producing accurate uranium isotopic information has not yet been rigorously interrogated. Here we present a method for producing rapid  $^{235}\text{U}/^{238}\text{U}$  ratios without the need for significant lab infrastructure. The success of this process is dependent upon both precise analytical optimization and robust data calibration. This

<sup>a</sup> Savannah River National Laboratory, Aiken, South Carolina 29808, United States of America

<sup>b</sup> Trace Nuclear Measurement Technology Group, Savannah River National Laboratory

contribution highlights ongoing efforts to develop, optimize, and operationalize MAI for trace-level uranium isotopic analyses.

## 2 Methods

### 2.1 Instrumentation and Materials

MAI experiments were performed using an atmospheric pressure ionization, time-of-flight JEOL AccuToF DART 4G mass spectrometer (JEOL, Peabody, MS, USA) run in negative ion mode at the Savannah River National Laboratory (SRNL). 3-nitrobenzonitrile (3-NBN, Sigma Aldrich, St. Louis, MO, USA) was chosen as the ionization matrix based on extensive use in published literature and its success in ionizing a variety of analytes<sup>18,37,38</sup>. Fomblin Y (HVAC 16/6, Sigma Aldrich, St. Louis, MO, USA) was run at the conclusion of each analysis series using a DART ion source to calibrate instrumental mass spectra<sup>18</sup>. Additional instrument parameters are detailed in the Supporting Information. New Brunswick Laboratory Certified Reference Materials (CRMs, NBL Program Office, Oak Ridge, TN, USA) of uranium oxide isotopic standards dissolved in 2% nitric acid were utilized for analysis: CRM U020 ( $\approx 2\%$   $^{235}\text{U}$ ), CRM U010 ( $\approx 1\%$   $^{235}\text{U}$ ), CRM C129 ( $\approx 0.7\%$   $^{235}\text{U}$ ), and CRM U005 ( $\approx 0.5\%$   $^{235}\text{U}$ ). These standards encompass  $^{235}\text{U}$  contents spanning slightly depleted to low enriched uranium, thus testing the analytical capability of the mass spectrometer across a compositional range pertinent to nuclear safeguards verification.

### 2.2 Experimental Configuration and Optimization

Sample solutions were prepared by combining  $\approx 10$  mg of 3-NBN, 50  $\mu\text{L}$  of methanol, and uranium standards in 2% nitric acid to yield a final sample volume of 100  $\mu\text{L}$ . This resulted in samples containing 1:1 methanol: 2% nitric acid for MAI analysis. Discrete runs for each CRM standard consisted of analyzing a reagent blank followed by prepared solutions of progressively higher uranium concentration, consisting of: 0 ng/g (reagent blank), 1 ng/g, 2.5 ng/g, 5 ng/g, 10 ng/g, 15 ng/g, 25 ng/g, 50 ng/g, 75 ng/g, and 100 ng/g. Consistent with previous observations<sup>18</sup>, the dominant uranium ion observed in negative ion mode for this sample preparation workflow was uranyl trinitrate,  $[\text{UO}_2(\text{NO}_3)_3]^-$ , with  $x = 5$  for  $^{235}\text{U}$  (452.99720 m/z) and  $x = 8$  for  $^{238}\text{U}$  (456.00407 m/z). The standard-methanol-3-NBN solution was vigorously agitated with a test tube shaker immediately prior to analysis to suspend 3-NBN crystals in solution. Sample uptake and introduction were accomplished by immersing a 5  $\mu\text{L}$  capillary tube (DWK Life Sciences, Millville, NJ, USA) into the analytical solution and subsequently allowing the negative pressure of the mass spectrometer orifice entrance to ambiently extract the sample.

Several sample introduction methods were evaluated to achieve the greatest signal intensity, including assessing the angle-of-incidence of the capillary tube and instrument orifice using both a stationary stage and manual introduction (Supplementary Fig. S1). Manually positioning the capillary tube slightly from the vertical and horizontal achieved the highest signal response. The parameter switching function in the instrument software allowed for the orifice and ring lens voltages to be sequen-

tially tested and optimized. These parameters were explored by running triplicate measurements of 10 ng/g, 25 ng/g, and 100 ng/g NBL CRM U020 standards. Counting the number of sample aspirations that produced a measureable and relatively accurate isotopic ratio at orifice 1 voltages ranging from -20 V through -150 V revealed -70 V as the optimal value (Supplementary Fig. S2). Ring lens voltage tests ranging from -5 V through -20 V demonstrated between -5 through -10 V as the optimal value. Orifice temperature experiments from 25-150  $^{\circ}\text{C}$  also exhibited a large effect on signal transmission, with the best sensitivity at 100-125  $^{\circ}\text{C}$  (Supplementary Fig. S3). As noted in previous studies<sup>18</sup>, the sample introduction process creates a spray of solution on the inside of the orifice which interferes with subsequent lower concentration analyses. To mitigate this instrument memory effect, the ion source vacuum region of the instrument was vented between each sample series to remove the external orifice, ring lens, and internal orifice. These components were cleaned with swabs dipped in 2% nitric acid and methanol before subsequent reinstallation and evacuation of the ion source region.

### 2.3 Data Analysis and Calibration

Data analysis was performed with the open-source R statistical programming language<sup>39</sup> using minimally processed, instrument-output NetCDF (.cdf) files. A minimum uranium isotopic measurement acceptance threshold was set to require  $\geq 3$  consecutive measurements for both the major and minor isotope masses per sample introduction; if  $< 3$  measurements were recorded for either isotope, the data was excluded from the isotopic ratio calculation. A measurement accuracy and precision assessment was performed to determine the optimal approach for calculating  $^{235}\text{U}/^{238}\text{U}$  using relative  $[\text{UO}_2(\text{NO}_3)_3]^-$  signal intensities. A weighted-mean isotope ratio and uncertainty calculation<sup>40</sup> consistently yielded the most accurate and repeatable (noncalibrated)  $^{235}\text{U}/^{238}\text{U}$  measurements, compared to arithmetic mean and peak-integrated calculations. An initial  $^{235}\text{U}/^{238}\text{U}$  isotope ratio calibration approach was implemented wherein primary standard (PS) analyses of CRM U020 are used to establish method traceability for secondary standard (SS) analyses of CRMs U005, C129, and U010.

## 3 Results and Discussion

### CRM U020 Measurement

Utilizing the optimized ToF-MS method permitted resolution of individual isotopic  $^{235}\text{U}$  and  $^{238}\text{U}$  signals from uranium concentrations at least as low as 5 ng (Fig. 1). While the ToF mass analyzer allowed simultaneous detection of all ions, the limited (3 orders of magnitude) dynamic range of the AccuToF detector resulted in the exclusion of any isotopes that were  $< 0.1\%$  abundant. This aspect of the instrument prevented the lesser-abundant  $^{234}\text{U}$  and  $^{236}\text{U}$  isotopes ( $\approx 0.01$ - $0.02\%$  in U020) from being quantified. Although the  $^{235}\text{U}/^{238}\text{U}$  relative uncertainties for 5-500 ng mass loads of CRM U020 range from 17-1% weighted relative standard error (RSE), respectively, their offset from the certified value ranged from 3 to 48%. These results were observed to be more accurate than non-weighted values, which exhibited up to

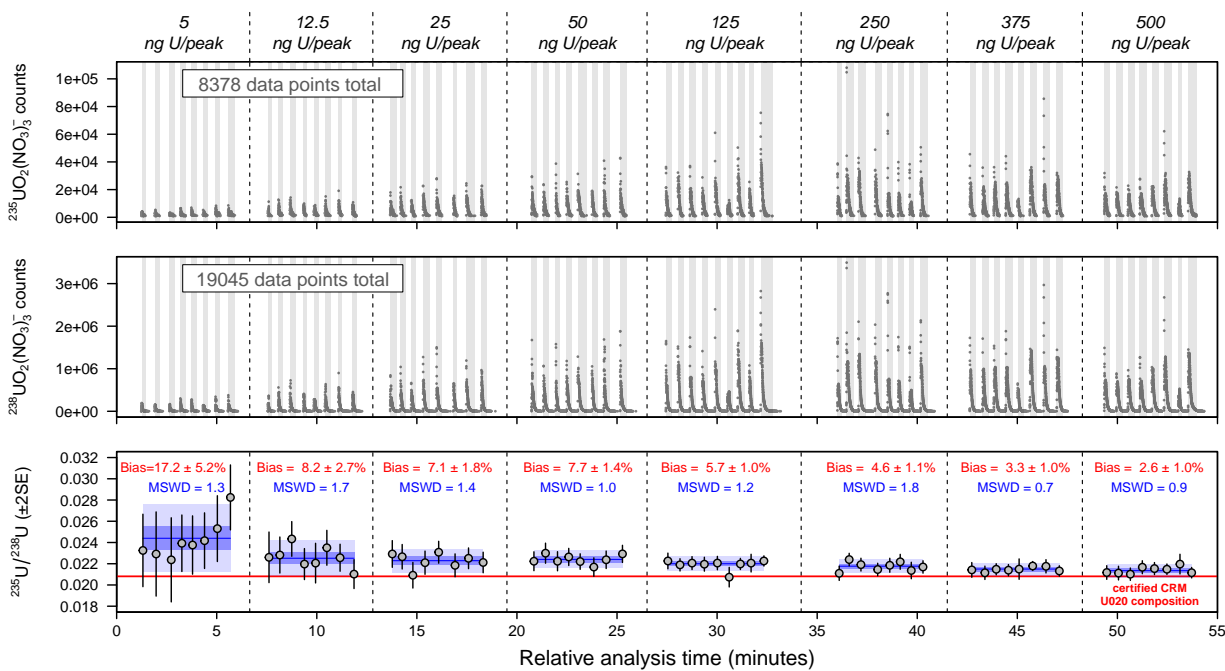


Fig. 1 Extracted ion chromatogram (EIC) time-series from MAI analysis of CRM U020, binned by maximum U amount, showing  $^{235}\text{UO}_2(\text{NO}_3)_3^-$  signal (top),  $^{238}\text{UO}_2(\text{NO}_3)_3^-$  signal (middle), and  $^{235}\text{U}/^{238}\text{U}$  isotope ratios and uncertainties (2SE) for individual analytical aliquots/EIC peaks (bottom). Light blue bands: average uncertainties of individual measurements within each bin. Dark blue bars: uncertainties associated with pooled measurements for each bin. Measured  $^{235}\text{U}/^{238}\text{U}$  bias from the certified CRM U020 value decreases from left-to-right.

60% bias from the certified isotopic ratios.

In addition to the accuracy and precision of individual measurements, repeatability of compositionally-identical measurements throughout an analysis sequence was used to assess the ability of the instrument to produce reliable data. To this end, the data were binned based on uranium concentration in order to compare the goodness-of-fit of multiple analyses of similar analyte concentration to their weighted mean value (Fig. 1). An especially effective metric for determining if a set of analyses and associated analytical uncertainties are statistically consistent with derivation from a singular normal distribution is the reduced chi-squared statistic, also known in the natural sciences as the mean square weighted deviation (MSWD), which is calculated by dividing the chi-squared statistic by the degrees of freedom<sup>40</sup> ( $n-1$ ). At the 95% confidence level, an  $\text{MSWD}=1$  suggests measurement variance is accurately captured by the analytical uncertainties;  $\text{MSWD}<1$  is indicative of an overestimation of analytical uncertainties; and an  $\text{MSWD}>1$  suggests uncertainties were underestimated or that the analyses represent a heterogeneous material<sup>40</sup>. Furthermore, the dependence of the MSWD statistic on the degrees of freedom allows the above criteria to be adjusted based on sample number<sup>40</sup>. Despite the overall large bias between individual measurements and certified values, measurements binned by uranium concentration had MSWDs consistently  $<2$  at a 95% confidence level for all concentration bins, indicating the calculated uncertainty estimates accurately encapsulated the precision of the system and were consistent with counting statistics given the pertinent degrees of freedom<sup>40</sup>. Binning data has the added benefit of decreasing overall uncertainty via effectively increas-

ing signal integration, as illustrated by the averaged individual uncertainties (light blue) and much more precise binned data uncertainty (dark blue) in Fig. 1. We note that semi-quantitative sample uptake and introduction to the instrument require that reported mass loading concentrations are theoretical maximum values. This need to approximate concentration was primarily driven by two factors: 1) qualitative sample volume loading into the 5  $\mu\text{L}$  capillary, and 2) the heterogeneous 3-NBN crystal distribution in the sample solution.

#### Uranium Isotopic Calibration

Exploring a range of uranium concentrations from 5-500 ng revealed that the  $^{235}\text{U}/^{238}\text{U}$  measurement was systematically biased towards higher values, the magnitude of which was inversely proportional to signal intensity, i.e., uranium concentration, such that pooled bias ranged from  $17.2 \pm 5.2\%$  for a 5 ng load through  $2.6 \pm 1\%$  for a 500 ng load (Fig. 1, 2).

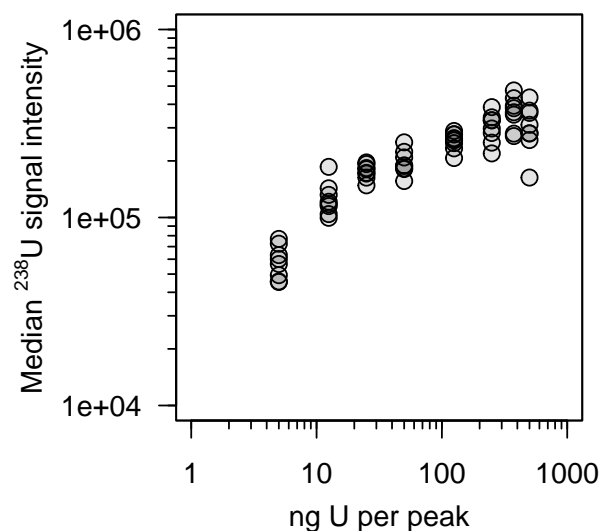


Fig. 2 Median  $^{238}\text{U}$  signal intensity (counts) as a function of uranium mass (nanograms) per individual analytical aliquot/EIC peak. Data are the same CRM U020 analyses as in Figure 1.

We hypothesize that this bias arises from an unresolved isobaric interference at  $m/z = 452.99720$  (corresponding to the  $^{235}\text{UO}_2(\text{NO}_3)_3^-$  mass peak) which was inherently more pronounced at lower uranium concentrations and thus trended towards higher measured  $^{235}\text{U}/^{238}\text{U}$  values. This bias was exacerbated through the algorithm by which the native MS software converts the full scan mass spectrum to a centroid spectrum using peak width. Thus, isobaric interferences that broadened peak width were incorporated into the centroid spectra and increased the apparent  $^{235}\text{U}$  mass signal. This effect required a more nuanced calibration to capture the concentration-dependent nature of the  $^{235}\text{U}/^{238}\text{U}$  measurement than a simple linear fit approach. Instead, the positively-skewed bias produced from analyses spanning a range of standard concentrations resulted in a curve that can be modelled by fitting the measured data to a relatively simple exponential function:

$$y = Ae^{-Bx} \quad (1)$$

where  $x$  = median  $^{235}\text{U}$  signal intensity and  $y$  = measured  $^{235}\text{U}/^{238}\text{U}$  (Fig. 3, panel A). A least-squares, Monte Carlo-based fitting of the U020 data resulted in exponential curve constants  $A = 0.02412 \pm 0.00084$  and  $B = 1.47 \pm 0.52 \text{ e}^{-5}$  with a correlation of  $r_{AB} = -0.99$ . This very strong correlation suggests the model accurately captures the relationship between measured isotope ratio bias and signal intensity. Weighted mean  $^{235}\text{U}/^{238}\text{U}$  ratios of U010 and other secondary standards exhibit an analogous inverse relationship between isotope ratio bias and signal intensity of equal magnitude to U020 (Fig. 3, panel B for U010), which suggests the same process affects measurement bias across different samples.

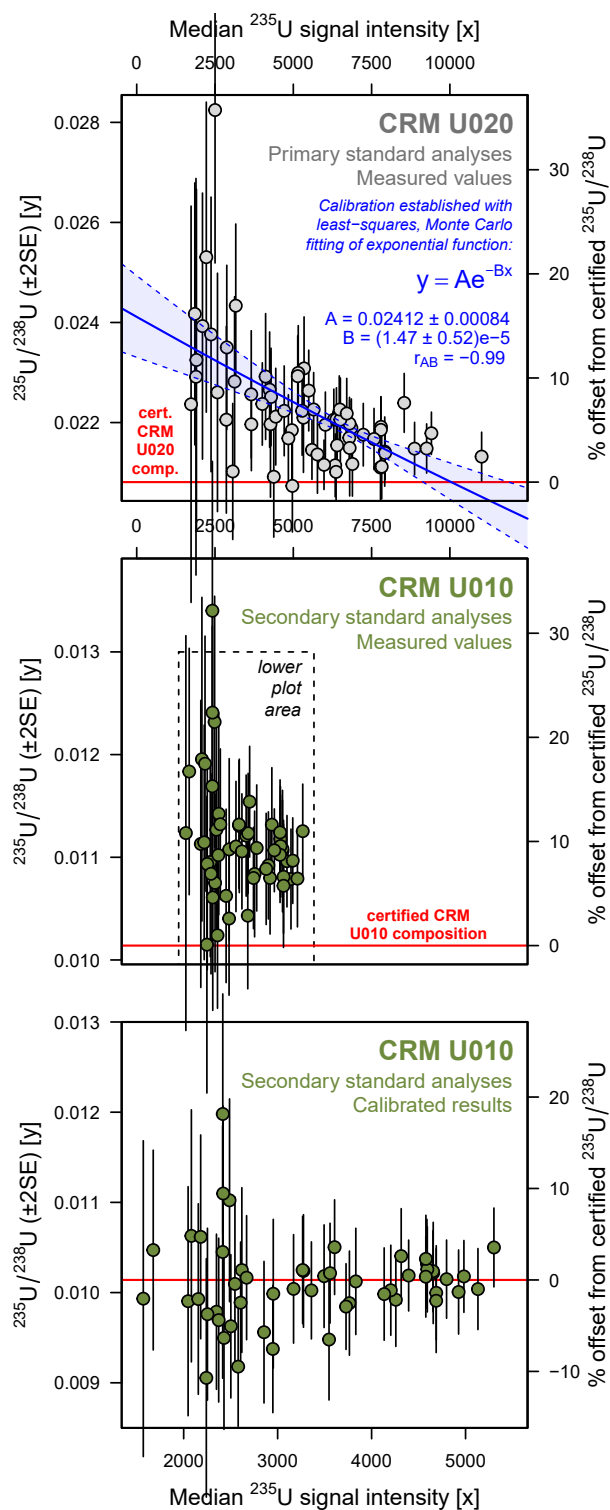


Fig. 3  $^{235}\text{U}/^{238}\text{U}$  calibration for MAI uranium isotopic analysis. CRM U020 data (same as Figures 1 and 2) quantifies dependence of measured  $^{235}\text{U}/^{238}\text{U}$  as a function of median  $^{235}\text{U}$  signal intensity (top). The  $^{235}\text{U}$  intensity-based calibration curve is applied to measured secondary standard CRM U010 data (middle) to calculate calibrated  $^{235}\text{U}/^{238}\text{U}$  results (bottom). Uncertainties in top and middle panels are weighted 2SE calculations, and individual measurement uncertainties in the bottom panel are combined uncertainties propagated from measurement and calibration, resulting in externally traceable uncertainty estimation.

Measured median  $^{235}\text{U}$  of secondary standards analyses were

then applied to x in Equation 1 to obtain a “measured”/applied U020  $^{238}\text{U}/^{235}\text{U}$  value for use in Equation 2, which returns a corrected  $^{235}\text{U}/^{238}\text{U}$  value for each measured ratio. This “measured”/applied U020 value is then inserted into the following calibration equation:

$$\left(\frac{^{235}\text{U}}{^{238}\text{U}}\right)_{SS_{cal}} = \left(\frac{^{235}\text{U}}{^{238}\text{U}}\right)_{SS_{meas}} \left(\frac{^{238}\text{U}}{^{235}\text{U}}\right)_{PS_{meas}} \left(\frac{^{235}\text{U}}{^{238}\text{U}}\right)_{PS_{cert}} \quad (2)$$

In Equation 2, the leftmost term is the *calibrated*  $^{235}\text{U}/^{238}\text{U}$  of a SS analysis (U005, C129, or U010). The three terms at right correspond, from left-to-right: 1) the *measured* SS  $^{235}\text{U}/^{238}\text{U}$ ; 2) the “measured”/applied PS (U020)  $^{238}\text{U}/^{235}\text{U}$ ; and 3) the *certified* PS  $^{235}\text{U}/^{238}\text{U}$  (i.e., the certified composition of the PS through which  $^{235}\text{U}/^{238}\text{U}$  metrological traceability is established). Due to percent-level  $^{235}\text{U}/^{238}\text{U}$  measurement uncertainty currently characteristic of MAI uranium analysis, the uncertainty contribution of the certified  $^{235}\text{U}/^{238}\text{U}$  of the U020 PS (ca.  $\pm 0.1\%$  at 95% CL) is insignificant and thus omitted during uncertainty propagation. This signal intensity-based calibration approach effectively corrects otherwise heavily biased secondary standard values (Fig. 3, panel B) to within their certified value (Fig. 3, panel C).

The above process was applied to a range of secondary standard uranium concentrations and compositions, spanning depleted to slightly enriched in  $^{235}\text{U}$ : CRM U005 with 0.5%  $^{235}\text{U}$ , CRM C129 with 0.7%  $^{235}\text{U}$ , and CRM U010 with 1%  $^{235}\text{U}$ . This analysis and calibration technique reproduced the certified  $^{235}\text{U}/^{238}\text{U}$  values for all uranium compositions and concentrations with a weighted mean uncertainty as low as 1.5% (Fig. 4). To emphasize the significance of this result, with an analysis time of only  $\approx 5$  seconds per sample, all three uranium enrichment compositions (which vary only slightly in  $^{235}\text{U}$  composition by 0.2–0.3%) can be distinguished and accurately characterized. The success of this model illustrates how the measured MAI data was consistently biased in a predictable, measurable, and correctable fashion, regardless of the amount or isotopic composition of sample analyzed.

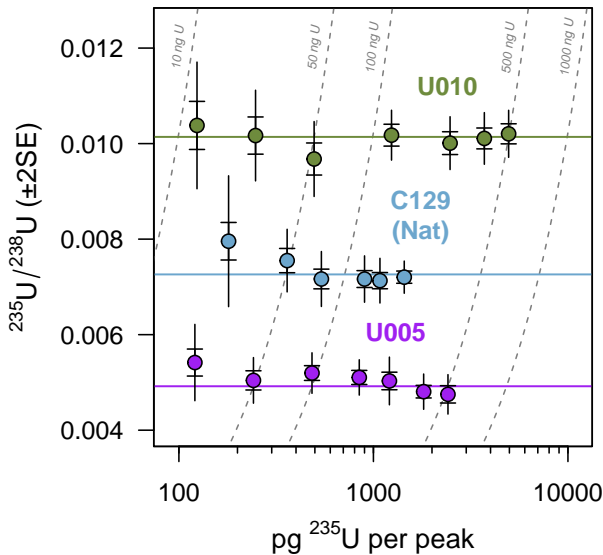


Fig. 4 Secondary standard summary of calibrated, mean  $^{235}\text{U}/^{238}\text{U}$  binned values as a function of  $^{235}\text{U}$  mass (picograms) per individual analysis/EIC peak. Solid horizontal lines indicate certified  $^{235}\text{U}/^{238}\text{U}$  values. Dashed grey contours indicate maximum U mass (nanograms) per analysis. Large/uncapped uncertainties are mean individual measurement values; small/capped uncertainties are integrated weighted-mean values for all measurements in a bin.

A significant aspect of this calibration approach was the ability to predict the behavior of low mass or poorly-transmitted analyses and effectively correct for high  $^{235}\text{U}/^{238}\text{U}$  bias, returning a sample measurement to within certified isotope ratio values. We note that this approach yields a concentration-independent correction factor, which presents a unique advantage for scenarios where sample loading is variable and/or unstable. An additional advantage of this technique is the ability to reliably analyze uranium compositions at the extreme limit of the instrument’s detection capabilities. Under current optimization settings of the microchannel plate detector (MCP) on SRNL’s JEOL AccuToF, a significant but definable noise floor defines a detection limit of approximately 1000 cps; this detection limit requires a minimum mass of  $\approx 100$  pg of an individual uranium isotope species for detection. Therefore, when measuring equal atom  $^{235}\text{U}:^{238}\text{U}$  (e.g., 50%  $^{235}\text{U}$ , not empirically evaluated here), this calibration approach could recover the certified value with a mass loading as low as 200 pg total uranium (Fig. 5). The applicability of this analysis method within nuclear safeguards can be further extended by leveraging the detection limit of the instrument against  $^{235}\text{U}$  enrichment. In the absence of the less abundant  $^{235}\text{U}$  signal due to low uranium concentration, knowledge of the instrument’s detection limit permits determination of a maximum permissible  $^{235}\text{U}/^{238}\text{U}$  ratio given a  $^{238}\text{U}$  signal above background (Fig. 5, panel A). For example, such an approach allows us to constrain whether a sample surpasses the low-enriched uranium (LEU)-to-highly-enriched uranium (HEU) transition (defined as 20%  $^{235}\text{U}$ ) even in the absence of detectable  $^{235}\text{U}$ ; if  $^{238}\text{U}$  intensity is  $\geq 4000$  cps, then an LEU vs. HEU assessment can be made given as little



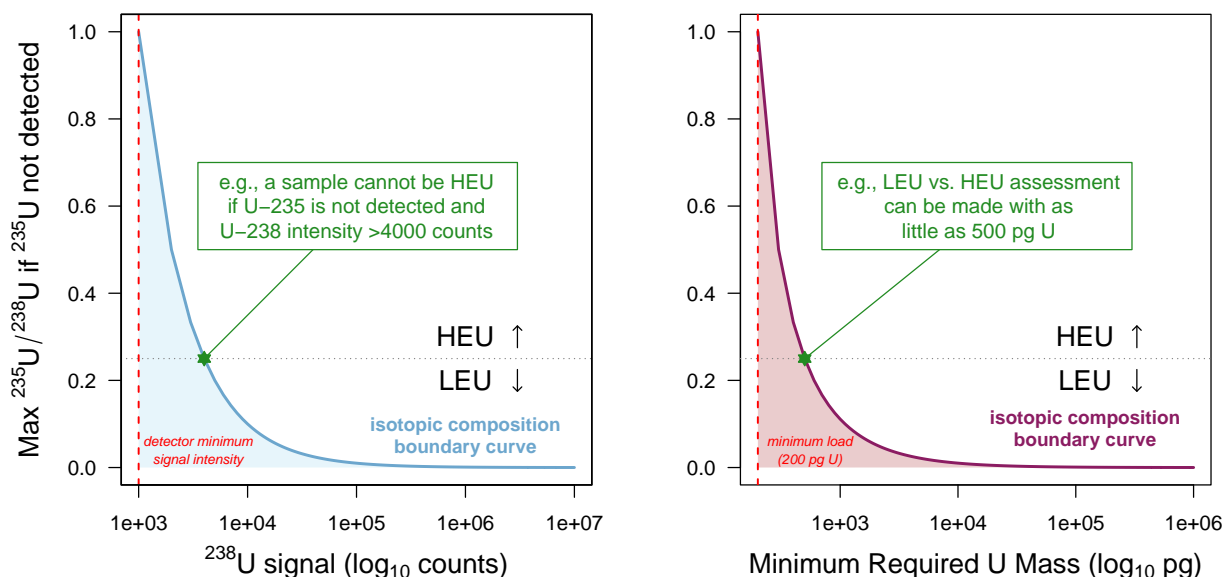


Fig. 5 Panel A) Maximum permissible  $^{235}\text{U}/^{238}\text{U}$  ratio if  $^{235}\text{U}$  is not detected as a function of  $^{238}\text{U}$  cps or the JEOL ToF instrument (detection limit = 1000 cps using optimized instrument settings). Green star: transition from low-enriched uranium (LEU)-to-highly-enriched uranium (HEU), with  $^{238}\text{U}$  signal intensity of  $\geq 4000$  cps and non-detection of  $^{235}\text{U}$ . Panel B) Maximum permissible  $^{235}\text{U}/^{238}\text{U}$  ratio given a minimum total uranium mass in picograms, highlighting the ability to detect a sample at the LEU-HEU transition with 500 pg total uranium.

as  $\approx 500$  pg total uranium (Fig. 5, panel B). Such a capability is crucial for potential nuclear safeguards verification, e.g., enabling an inspection agency to confidently and rapidly verify compliance of declared facilities even given a “non-detect” for  $^{235}\text{U}$  in a low-level environmental sample.

## Conclusions

This work presents the first demonstration of quantitative uranium isotopic analysis using MAI ambient mass spectrometry. We establish that MAI-ToF-MS holds promise as a rapid and cost-effective method to produce accurate uranium isotopic measurements without the need for significant lab infrastructure. Through a combination of instrument parameter optimization and data calibration using Certified Reference Materials, we demonstrated accurate  $^{235}\text{U}/^{238}\text{U}$  values for secondary standards in concentrations spanning 5-500 ng for a range of uranium enrichments. This approach produces weighted mean uncertainties approaching 1.5% and is applicable to uranium compositions from LEU through HEU and concentrations as low as 200 pg for equal atom  $^{235}\text{U}/^{238}\text{U}$  uranium compositions. Future work will incorporate the developed isotopic calibration method into a customized graphical user interface (GUI) for simple “point-and-click” data analysis.<sup>41</sup> Additionally, uranium-bearing environmental sample surrogates (e.g., environmental sampling swipes) will be analyzed using MAI-ToF-MS to further characterize the method’s applicability to environmental matrices. Finally, MAI uranium isotopic analysis will be evaluated using alternative mass spectrometer platforms to assess the viability of accurately quantifying minor isotopes (e.g.,  $^{234}\text{U}$  and  $^{236}\text{U}$ ) that are too low to be detected given the limited dynamic range of a ToF mass analyzer.

## Author contributions

**Shelby Bowden:** Software, Formal Analysis, Data Curation, Writing - Original Draft, Visualization; **Kyle Samperton:** Conceptualization, Methodology, Software, Validation, Formal Analysis, Data Curation, Writing - Review & Editing, Visualization; **Elizabeth D. LaBone:** Software, Formal Analysis, Data Curation, Visualization, Writing - Review & Editing; **Haley B. Lawton:** Investigation; **Abigail M. Waldron:** Investigation; **Joseph M. Mannion:** Conceptualization, Methodology, Writing - Review & Editing; **Matthew S. Wellons:** Conceptualization, Resources, Funding Acquisition; **Danielle R. Mannion:** Conceptualization, Methodology, Software, Validation, Formal Analysis, Investigation, Resources, Data Curation, Writing - Review & Editing, Supervision, Project Administration, Funding Acquisition.

## Conflicts of interest

There are no conflicts to declare.

## Data availability

The data that support the findings of this study are included in the supplementary information.

## Acknowledgements

This work was produced by Battelle Savannah River Alliance, LLC under Contract No. 89303321CEM000080 with the U.S. Department of Energy. Publisher acknowledges the U.S. Government license to provide public access under the DOE Public Access Plan (<http://energy.gov/downloads/doe-public-access-plan>). This work was supported by the U.S. Department of Energy, National Nuclear Security Administration (NNSA), Office

of Defense Nuclear Nonproliferation Research and Development (DNN R&D) under project number SR21-MAIV-MS-PD3Ha. The authors thank Sarah Trimpin, Chuck McEwen, KateLyn Smith, and Chip Cody for their support and assistance.

Notes and references

1 J. Becker, M. Zoriy, L. Halicz, N. Teplyakov, C. Muller, I. segal, C. Pickhard and I. Platzner, *Journal of Analytical Atomic Spectrometry*, 2004, **19**, 1257–1261.

2 J. Zheng, K. Tagami, Y. Watanabe, S. Uchida, T. Aono, N. Ishii, S. Yoshida, Y. Kubota, S. Fuma and S. Ihara, *Scientific Reports*, 2012, **2**,.

3 M. Wallenius and K. Mayer, *Fresenius Journal of Analytical Chemistry*, 2000, **366**, 234–238.

4 K. Mayer, M. Wallenius and I. Ray, *Analyst*, 2005, **130**, 433–441.

5 D. Donohue, *Journal of Alloys and Compounds*, 1998, **271-273**, 11–18.

6 S. Boulyga, S. Konegger-Kappel, S. Richter and L. Sangely, *Journal of Analytical Atomic Spectrometry*, 2015, **30**, 1469–1489.

7 S. Richter and S. A. Goldberg, *International Journal of Mass Spectrometry*, 2003, **229**, 181–197.

8 S. Richter, H. Kühn, Y. Aregbe, M. Hedberg, J. Horta-Domenech, K. Mayer, E. Zuleger, S. Bürger, S. Boulyga, A. Köpf, J. Poths and K. Mathew, *Journal of Analytical Atomic Spectroscopy*, 2011, **26**, 550–564.

9 J.-F. Wotzlaw, Y. Buret, S. J. E. Large, D. Szymanowski and A. von Quadt, *Journal of Analytical Atomic Spectrometry*, 2017, **32**, 579–586.

10 F. Albarède, P. Telouk, J. Blichert-Toft, M. Boyet, A. Agranier and B. Nelson, *Geochimica et Cosmochimica Acta*, 2004, **68**, 2725–2744.

11 A. D. Pollington, W. S. Kinman, S. K. Hanson and R. E. Steiner, *Journal of Radioanalytical and Nuclear Chemistry*, 2016, **307**, 2109–2115.

12 S. Boulyga, A. Koepf, S. Konegger-Kappel, Z. Macsik and G. Stadelmann, *Journal of Analytical Atomic Spectrometry*, 2016, **31**, 2272–2284.

13 H. Dion, L. Ackermann and H. Hill, *Talanta*, 2002, **57**, 1161–1171.

14 M. V. Stipdonk, V. Anbalagan, W. Chien, G. Gresham, G. Groenewold and D. Hanna, *Journal of the American Society for Mass Spectrometry*, 2003, **14**, 1205–1214.

15 S. Pasilis, A. Somogyi, K. Herrmann and J. Pemberton, *Journal of the American Society for Mass Spectrometry*, 2006, **17**, 230–240.

16 M. Luo, B. Hu, X. Zhang, D. Peng, H. Chen, L. Zhang and Y. Huan, *Analytical Chemistry*, 2010, **82**, 282–289.

17 C. Crawford, G. Fugate, P. Cable-Dunlap, N. Wall, W. Siems and H. Hill, *International Journal of Mass Spectrometry*, 2013, **333**, 21–26.

18 D. R. Mannion, J. M. Mannion, W. W. Kuhne and M. S. Wellons, *Journal of the American Society for Mass Spectrometry*, 2021, **32**, 8–13.

19 J. V. Goodwin, B. T. Manard, B. W. Ticknor, P. Cable-Dunlap and R. K. Marcus, *Microchemical Journal*, 2024, **196**, 109645.

20 J. Goodwin, B. Manard, B. Ticknor, P. Cable-Dunlap and R. Marcus, *Analytical chemistry*, 2023, **95**,.

21 J. Goodwin, B. Manard, B. Ticknor, K. Rogers, C. Hexel, P. Cable-Dunlap and R. Marcus, *Journal of Radioanalytical and Nuclear Chemistry*, 2023, **332**,.

22 J. Goodwin, B. Manard, B. Ticknor, P. Cable-Dunlap and R. Marcus, *Journal of Analytical Atomic Spectrometry*, 2022, **37**,.

23 H. Paing, B. Manard, B. Ticknor, J. Bills, K. Hall, D. Bostick, P. Cable-Dunlap and R. Marcus, *Analytical Chemistry*, 2020, **92**,.

24 R. Cody and J. Dane, *Rapid Communications in Mass Spectrometry*, 2014, **28**, 893–898.

25 R. Narayanan and T. PRadeep, *Analytical Chemistry*, 2017, **89**, 10696–10701.

26 K. Coopersmith, R. Cody, J. Mannion, J. Hewitt, S. Koby and M. Wellons, *Rapid Communications in Mass Spectrometry*, 2019, **33**, 1695–1702.

27 Z. Devereaux, C. Reynolds, J. Fischer, C. Foley, J. DeLeeuw, J. Wager-Miller, S. N. an Ken Mackie and S. Trimpin, *Analytical Chemistry*, 2016, **88**, 10831–10836.

28 S. Trimpin, *Rapid Communications in Mass Spectrometry*, 2018, **33**, 96–120.

29 E. Inutan and S. Trimpin, *Molecular and Cellular Proteomics*, 2013, **12**, 792–796.

30 S. Trimpin and E. Inutan, *Analytical Chemistry*, 2013, **85**, 2005–2009.

31 D. Woodall, B. Wang, E. Inutan, S. Narayan and S. Trimpin, *Analytical Chemistry*, 2015, **87**, 4667–4674.

32 X. Zhou, W. Zhang and Z. Ouyang, *TrAC Trends in Analytical Chemistry*, 2022, **149**, 116548.

33 B. Jiao, H. Ye, X. Liu, J. Bu, J. Wu, W. Zhang, Y. Zhang and Z. Ouyang, *Analytical Chemistry*, 2021, **93**,.

34 D. Snyder, C. Pulliam, Z. Ouyang and R. Cooks, *Analytical chemistry*, 2015, **88**,.

35 S. Trimpin and E. Inutan, *Journal of the American Society for Mass Spectrometry*, 2013, **24**,.

36 S. Chakrabarty, V. Pagnotti, E. Inutan, S. Trimpin and C. McEwen, *Journal of the American Society for Mass Spectrometry*, 2013, **24**,.

37 S. Trimpin, C. Lutomski, T. El-Baba, D. Woodall, C. Foley, C. Manly, B. Wang, C.-W. Liu, B. Harless, R. Kumar, L. Imperial and E. Inutan, *International Journal of Mass Spectrometry*, 2015, **377**, 532–545.

38 C. Lee, E. Inutan, J. Chen, M. Mukeyu, S. Weidner, S. Trimpin and C.-K. Ni, *Rapid Communications in Mass Spectrometry*, 2019, **35**,.

39 R Core Team, *R: A Language and Environment for Statistical Computing*, R Foundation for Statistical Computing, Vienna, Austria, 2023.

40 I. Wendt and C. Carl, *Chemical Geology (Isotope Geoscience Sec-*



tion), 1991, **86**, 275–285.

41 E. Labone, K. Samperton and D. Mannion, *2023 INMM and ESARDA Joint Annual Meeting*, 2023.

1  
2  
3  
4  
5  
6  
7  
8  
9  
10  
11  
12  
13  
14  
15  
16  
17  
18  
19  
20  
21  
22  
23  
24  
25  
26  
27  
28  
29  
30  
31  
32  
33  
34  
35  
36  
37  
38  
39  
40  
41  
42  
43  
44  
45  
46  
47  
48  
49  
50  
51  
52  
53  
54  
55  
56  
57  
58  
59  
60



Journal of Analytical Atomic Spectrometry (JAAS)

**Subject:** Data availability statement for “Rapid  $^{235}\text{U}/^{238}\text{U}$  Determination by Matrix Assisted Ionization-Time-of-Flight Mass Spectrometry”.

The data supporting this article have been included as part of the Supplementary Information.

Best Regards,  
Shelby Bowden, PhD  
Scientist  
Savannah River National Laboratory  
Email: [Shelby.bowden@srnl.doe.gov](mailto:Shelby.bowden@srnl.doe.gov)  
Phone: 839-465-0690